JOURNAL OF MATERIALS SCIENCE 23 (1988) 3711–3720

Hybrid ceramic matrix composites

K. P. GADKAREE, K. C. CHYUNG, M. P. TAYLOR
Research and Development Division, Corning Glass Works, Corning, New York 14831

A model hybrid glass-matrix composite has been studied. The system investigated was Corning Code 1723 glass matrix (an alkaline earth aluminosilicate glass) with silicon carbide whiskers and Nicalon® fibres. It was found that a 10 wt% whisker loading of the matrix gave optimum composite properties. The optimized hybrid composite, when compared to an optimized non-hybrid composite, showed increases in microcrack yield stress from 330 to 650 MPa, interlaminar shear strength from 47 to 130 MPa, and transverse strength from 12 to 50 MPa, while the ultimate strength decreased from 965 to 900 MPa.

1. Introduction

Hybrid composites, consisting of two or three different types of reinforcing fibres, have been studied in detail in polymer matrix composites [1–8]. The objective of hybridization is to optimize the composite in terms of cost and mechanical properties. Graphite fibres are strong, low density, and possess high elastic modulus but are expensive. Glass fibres are relatively cheap and possess higher fracture strain, but they have a low elastic modulus and high density. Combination of these two reinforcements in a composite thus gives an optimized composite in terms of mechanical properties and cost. Such hybrid composites are being used for various applications such as racing car bodies, helicopter blades and power boats.

In the glass and glass-ceramic matrix composites, Nicalon® silicon carbide continuous fibre is being extensively studied as a reinforcement [9–11]. In such composites the matrix has a significantly lower failure strain ($\sim 0.1\%$) compared to the fibre ($> 1\%$). This difference in failure strain results in matrix microcracks at a strain much lower than the ultimate failure strain of the composite. Fig. 1 shows the stress–strain curve of a typical composite. Beyond the microcrack point the composite consists of a severely cracked matrix held together by the fibres. At high temperatures the microcracking phenomenon leads to oxidation embrittlement problems [12]. Efforts are being made to solve the oxidation embrittlement problem, for example, by coating the fibres, but concerns about significant loss in stiffness and fatigue problems associated with cracking of the brittle matrix would probably limit the design stresses to a certain percentage of the microcrack stress or strain. Since the microcrack stress is significantly less than the ultimate strength of the composite, the high strength of the fibre is not fully utilized. The glass and glass-ceramic matrix composites also have the problems associated with the fundamental anisotropic nature of the composites, such as low transverse and interlaminar shear strengths. These problems severely limit the use of these materials.

Single crystal silicon carbide whiskers ($\sim 0.5\,\mu$m in diameter and 10 to 20 μm long) have been found to reinforce glass and glass–ceramic matrices very significantly [13–15]. Several fold improvements in strength, fracture toughness, moduli etc. have been obtained. A whisker reinforced glass or glass–ceramic is thus a stronger and tougher matrix for reinforcement with continuous fibres compared to a non-whisker containing glass or glass–ceramic. The microcrack yield point, the transverse strength and interlaminar shear strength of such a composite may be expected to be higher than an unreinforced glass or glass–ceramic matrix. This paper reports a model hybrid composite system consisting of a glass matrix (Corning code 1723 alkaline earth aluminosilicate), Nicalon® silicon carbide fibres (Nippon Carbon Co) and silicon carbide whiskers (ARCO SC-9). The objective of the work was to optimize this hybrid system with respect to processing parameters, whisker percentage, etc. in terms of mechanical properties; and to explain the behaviour of these systems. The knowledge gained from this study is applicable to other composite systems, including glass–ceramic matrix hybrid systems.

2. Theoretical

In this section the theoretical background underlying thermochemical properties exhibited by hybrid composites is presented. The effect of hybridization on various composite properties is predicted from theory.

2.1. Ultimate strength

In the glass or glass-ceramic matrix composites the ultimate strength is essentially the strength of the fibres given by Equation 1, since the matrix cracks extensively beyond the microcrack point

$$\sigma_{ult} = \sigma_f V_f \quad (1)$$

where σ_{ult} is the ultimate strength and σ_f the fibre strength. Incorporation of whiskers is not expected to change this situation. The type of chemical bonding between the fibre and the matrix is also not expected

0022–2461/88 $03.00 + .12

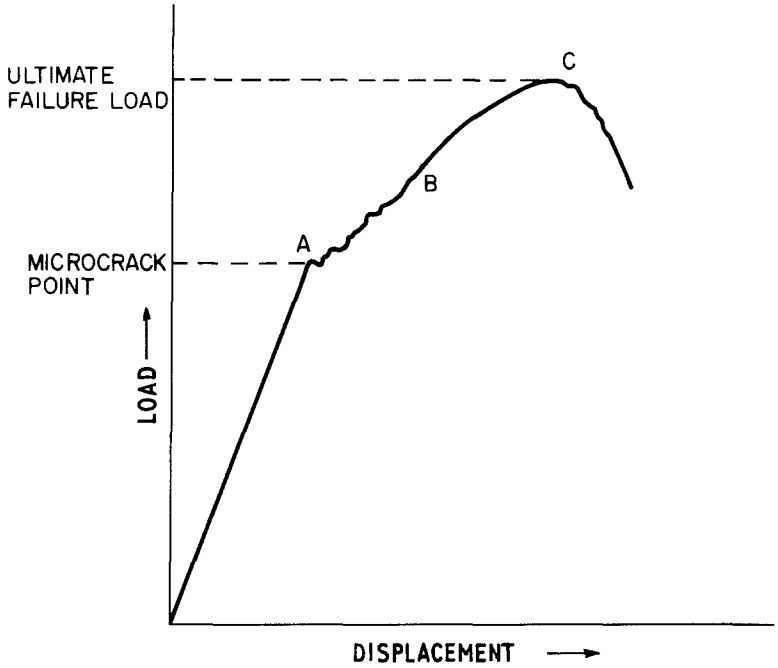

Figure 1 The load displacement relationship for a ceramic fibre–ceramic matrix composite.

to be affected. In that case the ultimate strength and the ultimate strain of the composite should be the same for conventional or hybrid composites, as long as the volume fraction of continuous fibres remains the same.

2.2. Microcrack stress and strain

The microcracking stress and strain are very important mechanical properties for the fibre composite. The microcracking strain and stress may be evaluated theoretically from the Aveston, Cooper and Kelly (ACK) theory for non-bonded [16] and well bonded [17] fibre–matrix composites. Details of the theories may be found in the respective references. In the following, the final equations for each of these models are presented.

2.2.1. ACK theory frictional bond case

The microcracking stress associated with a frictionally bonded fibre–matrix system is given according to the ACK theory by

$$\varepsilon_{mu} = \left(\frac{12\tau\gamma_m E_f V_f}{E_c E_m^2 r_f V_m}\right)^{1/3}$$

where ε_{mu} is the matrix microcracking strain, τ the interfacial shear stress, γ_m the matrix fracture energy, E_f, E_c and E_m the modulus of fibre, composite and matrix respectively, V_f and V_m the volume fractions of fibre and matrix respectively and r_f the radius of the fibre.

In this equation all the terms except the interfacial shear strength are easily measurable. Assuming that the interfacial shear strength remains the same after hybridization, we obtain

$$\frac{\varepsilon_{mu_1}}{\varepsilon_{mu_2}} = \left(\frac{E_{c_2} Em_2^2 \gamma_{m_1}}{E_{c_1} Em_1^2 \gamma_{m_2}}\right)^{1/3} \quad (2)$$

where the subscripts 1 and 2 refer to before and after hybridization.

The assumption of a constant interfacial shear strength is reasonable, since the chemistry of the interface is not expected to change.

2.2.2. ACK bonded case

The ACK theory for the case where fibres and matrix are well bonded gives the following equation for matrix microcrack stress

$$\varepsilon_{mu}^2 = \frac{2\gamma_m V_m}{r_f \alpha E_c}\left(\frac{2G_m E_c}{\Psi E_f V_m E_m}\right)^{1/2} \quad (3)$$

where G_m is the matrix shear modulus, Ψ the geometry factor and

$$\alpha = \frac{E_m V_m}{E_f V_f}$$

The change in microcrack strain may thus be obtained from the following equation

$$\frac{\varepsilon_{mu_1}^2}{\varepsilon_{mu_2}^2} = \frac{\gamma_{m_1} E_{m_2}}{\gamma_{m_2} E_{m_1}}\left(\frac{G_{m_1} E_{m_2} E_{c_2}}{G_{m_2} E_{m_1} E_{c_1}}\right)^{1/2} \quad (4)$$

In deriving Equation 4 from Equation 3, no assumption has been made except that the geometrical arrangement of fibres in the matrix remains the same in both the fibre and the hybrid composites.

Fig. 2 shows the variation of the microcracking stress with the addition of increasing percentage of whiskers in the matrix. Both the ACK non-bonded and bonded theories have been used in the analysis, because of the existing debate about the nature of the bond in the glass–SiC fibre composites. (Mandell [18] *et al.* have shown that the bond is much stronger than frictional type of weak bonding.)

Both of the theories predict significant increases in the microcrack yield point with increasing whisker percentage in the matrix. The well bonded composite systems will benefit much more than the non-bonded systems, due to the presence of the whiskers in the matrix.

Matrix fracture energy is thus the controlling parameter in microcrack yielding. Therefore, increases in the whisker percentage lead to increases in microcrack

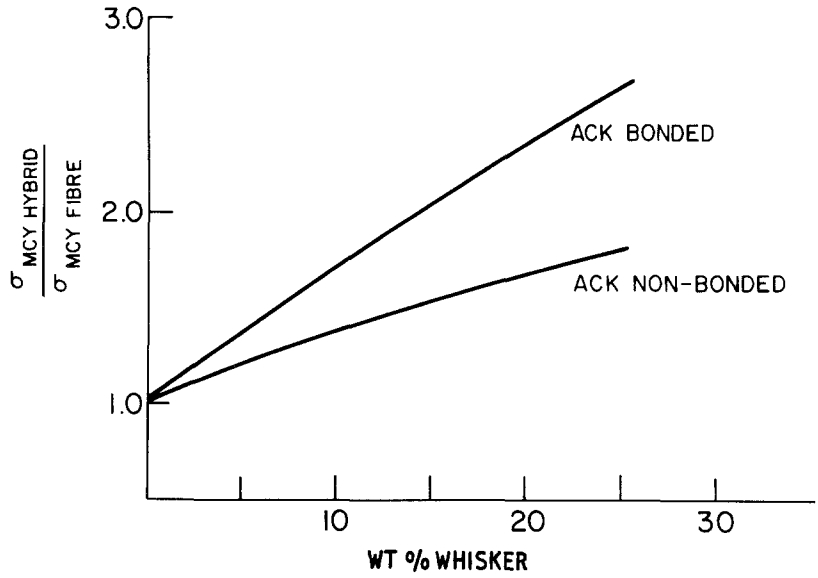

Figure 2 Variation of microcrack stress as a function of whisker percentage in hybrid composites.

yield point, because addition of whiskers raises the fracture toughness of the matrix. There would, however, be a limit to the maximum percentage of whiskers that can be added to the matrix. This limit will be determined by two factors. The first factor is the modulus of the whisker reinforced glass or glass-ceramic. A Young's modulus of 186 GPa has been measured for a 30 wt % whisker reinforced cordierite glass ceramic. The "Nicalon"® fibre has a modulus of 207 GPa. Thus, at very high whisker loadings the desired load transfer from matrix to the fibres may not take place in certain matrices. The whisker percentage would thus have to be optimized for a given fibre–matrix system. The second factor is that of the processing limitations of the fibre composites. Addition of whiskers results in very significant viscosity increases at processing temperatures. Increases in processing temperature to compensate for higher viscosity may lead to deterioration of the Nicalon® fibre. Since a well consolidated composite is desired to obtain the maximum benefit out of hybridization, the percentage of whiskers that can be incorporated in a hybrid composite would be limited. These two factors then would determine the optimum whisker percentage in a given fibre–matrix system.

2.3. Transverse strength

The transverse strength is determined by the matrix strength and the interfacial bond strength, assuming that the composites are well consolidated. Since increase in whisker percentage increases the matrix strength, the transverse strength of the hybrids is expected to increase with increases in whisker percentage. Prediction of the transverse strength may be carried out by an empirical approach using the following equation [19]

$$\sigma_{ct} = \sigma_m \frac{E_{tc}(1 - v_f^{1/3})}{E_m} \quad (5)$$

matrix strength, E_{tc} the composite transverse modulus where σ_{ct} is the composite transverse strength, σ_m the and E_m the matrix modulus. E_{tc} may be obtained from

$$E_{tc} = \frac{1}{\sum_{i=1}^{n} V_i/E_i} \quad (6)$$

The transverse strength of the composites may also be predicted by using one of two methods: (1) the strength of materials method; or (2) the advanced elasticity method using numerical solution techniques. In both methods it is assumed that the composite transverse strength is controlled by the matrix strength. It is further assumed that the composite strength is obtained from matrix strength by the equation

$$\sigma_{ct} = \frac{\sigma_m}{S} \quad (7)$$

where S is called the strength reduction factor, and is a function of fibre volume fraction and relative properties of the matrix and the fibre. We shall consider only the simpler strength of material method, where S is assumed to be the stress concentration factor (SCF) given by [20]

$$\text{SCF} = \frac{1 - V_f(1 - E_f/E_m)}{1 - (4V_f/\pi)^2(1 - E_f/E_m)}$$

Fig. 3 also shows the expected variation of transverse strength according to Equation 5 and Equation 7. Either approach predicts several fold increases in transverse strength with whisker reinforcement.

2.4. Interlaminar shear strength

The interlaminar shear strength of the composite, though an important property, is very difficult to predict. It is, however, known that the interlaminar shear strength of polymer composites increases with increases in tensile or shear strength of the matrix [20]. Based on this experimental evidence, it may be expected that the interlaminar shear strength will increase with increasing whisker percentage.

2.5. Theoretical conclusions

The above considerations result in the following conclusions regarding the behaviour of hybrid composites.

(1) The ultimate failure stress and strain of the composites should be the same for the hybrid system.

(2) Microcrack yield stress and strain could be increased significantly depending on the whisker content.

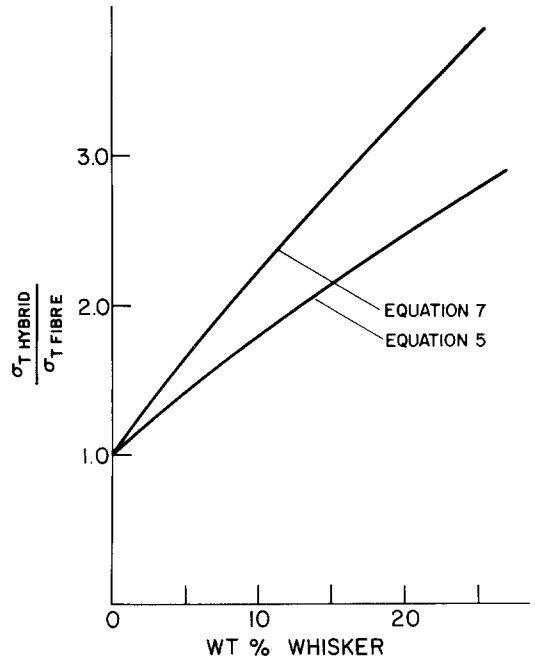

Figure 3 Variation of predicted transverse strength as a function of whisker percentage in the composite.

(3) Transverse and interlaminar shear strengths may also be expected to increase significantly.

(4) The optimum whisker percentage will be determined by a balance of mechanical and process considerations.

In the following, experimental results are described and compared with the theoretical predictions.

3. Materials and experimental

The material chosen for this study was Corning Code 1723 alkaline earth aluminosilicate glass, because of its ease of processing and possible wide variations in process conditions. The silicon carbide whiskers used were ARCO SC-9 whiskers and the fibres were silicon oxy carbide Nicalon NLM202 fibres made by Nippon Carbon.

The whiskers were mixed with glass powders by ball milling in isopropanol in appropriate proportions. The mixture was filtered and dried. The Nicalon fibres were then impregnated with this glass powder and whisker mixture using a polymeric binder system. The uniaxial prepregs were stacked, the binder burnt off at 450° C, and then hot pressed in graphite dies at various temperatures.

Composites were fabricated with 0 wt %, 5 wt %, 10 wt %, 18 wt % and 24 wt % SC-9 whisker and 1723 glass mixtures as matrices. The composites thus obtained were surface ground to 2 mm thickness and then cut on a diamond saw to 3.8 mm width. The ultimate stress and microcrack stress were measured on flexure bars. The bars were tested in four point flexure with 64 mm and 20 mm support and load spans. The transverse strength was also measured in four-point flexure on 40 mm and 20 mm spans. The interlaminar shear strength was measured by short beam shear or apparent interlaminar shear test, with a 6.4 mm span. Five specimens were measured under each condition to obtain the appropriate mechanical property value. Elastic modulus was measured by sonic resonance on a 13 mm × 3.17 mm × 101 mm composite specimen. Scanning electron microscopy of fractured and polished specimens was also carried out.

Tensile testing of the specimens was carried out as follows. Glass-reinforced epoxy tabs were bonded onto the straight sided specimens with epoxy. These specimens were equipped with strain gauges to measure microcrack and ultimate strains and stresses. Tensile elastic moduli were obtained from the initial linear portion of the curves.

All testing was done at 25° C.

4. Results and discussion

4.1. Ultimate strength and microcrack yield stress

Fig. 4 shows the variation in microcrack stress and ultimate strength of hybrid composites as a function of whisker content. Some very interesting observations may be made. Firstly, the composite ultimate strength decreases with increasing whisker percentage. Secondly, the microcrack stress has an optimum at 10 wt % whisker content. These two observations are contrary to the theoretical predictions of the previous section that the ultimate strength of the composite should remain the same for all hybrids, and that the microcrack stress should increase with increasing whisker percentage.

Fracture surface morphology also changes significantly with the addition of whiskers. Fig. 5a shows the fracture surface of a composite containing 0 wt % whisker. As expected, the fracture surface is very fibrous with long pullout lengths. The composite fails by fibre buckling on the compression surface. At 5 wt % whisker loading, however, the pullout lengths are reduced significantly as seen from Fig. 5b. Figs 5c, d, and e show the fracture surfaces of hybrid composites containing 10 wt %, 18 wt %, and 24 wt % whiskers. Pullout lengths decrease and the fracture surfaces becomes flatter with increasing whisker loading. Finally, at 24 wt % whisker loading there is almost no pullout. As seen from Fig. 4, the microcrack stress and the ultimate strength are the same for this (24 wt % whisker) composite.

4.2. Ultimate strength degradation and embrittlement

As mentioned before, two important points have to be explained: (1) the drop in the ultimate tensile strength of the composites with increase in volume fraction of whiskers; and (2) an optimum in the microcrack yield (mcy) stress, where a continuous increase in σ_{mcy} or mcy stress was expected with increasing whisker percentage. The changes in failure behaviour of the composites and the fracture surface morphology should also be explained.

The observed ultimate strength decrease with increase in whisker percentage may be due to one or more of the following reasons. Firstly, the whiskers which are hard and abrasive may damage the fibres during composite fabrication, resulting in fibre strength degradation. This would result in lower ultimate composite strengths. Secondly, due to the very high viscosities of whisker–glass slurries, compared to whisker-free slurries, the volume fraction of fibres in

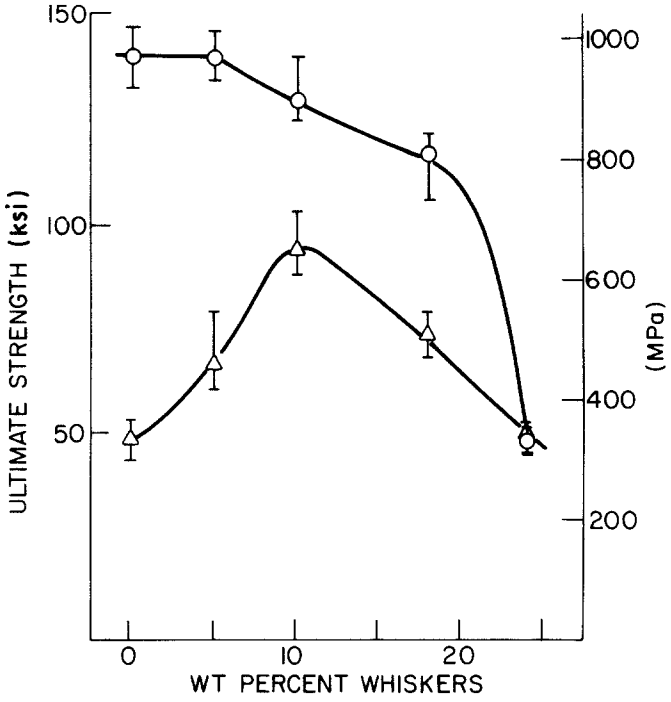

Figure 4 Ultimate strength (○) and microcrack stress (△) of the composites as a function of whisker percentage.

the hybrid composites may be lower than the volume fraction of fibres in the whisker-free composites. (This point was prompted by the observation of the prepreg winding process, where the amount of matrix material on the fibres appeared to be much higher for hybrid matrix than in the case of pure glass.) The decreased volume fraction of fibres would result in decreased ultimate strength of the composites. Thirdly, there may be a chemical variation in the interface structure, making the bonding stronger than optimum. Such composites would be brittle and, therefore, would be expected to have low strengths. Even though such a chemical variation of the interface structure is unlikely, the change in the fracture surface morphology with increasing whisker percentage suggests some type of embrittlement and, hence, this factor cannot be ruled out *a priori*. All the factors mentioned above are considered below in detail.

4.2.1. Chemical interface structure: Auger analysis

The hybrid composites at whisker loading levels of 0, 5, 10 and 24 wt % were analysed by scanning auger microscopy (SAM) at Physical Electronics Divison of Perkin Elmer. The experimental technique was to cut prisms of the composite measuring 2.5 mm × 2.5 mm × 12.7 mm, which were then coated with gold to insure good electrical conductivity. The prisms were cut such that the fibres were aligned with the short axis. The prism was mounted in a standard auger sample holder and broken in half under high vacuum in the auger. Because of the fibre alignment in the prism, the break occurred parallel to the fibre layers. This exposed some fibres and troughs where fibres had pulled away from the matrix.

The fibre–matrix interface was analysed by choosing points on a fibre and a trough and then collecting data after each of several sputtering treatments. The sputtering treatments are calibrated to remove a known amount of material from the surface, thus allowing a compositional profile into the depth of the fibre to be determined. The depth profiles are shown in Figs 6 and 7. In the depth profiles, negative values of the sputtering depth correspond to analyses taken on the fibre. In other words, the zero point on the sputtering depth axis may be taken as the fracture origin.

Despite the complex appearance of the SAM profiles, they are very similar. Firstly, failure always takes place at a carbon-rich interface, with relatively high carbon on the fibre side and low carbon on the matrix or trough side. Secondly, the carbon-rich zone on all the composites from this group was very thin, possibly as little as 10 nm. This contrasts with many glass–ceramic matrix composites where the zone may be several times thicker. Finally, matrix elements such as barium, calcium, and boron have diffused into the fibre to depths of 30–60 nm. It is speculated that this diffusion occurs prior to the formation of the carbon layer. Neither the depth of diffusion nor the concentration of diffused elements appears to be correlated with whisker content.

There are several significant differences among the four composites, but none appears to be correlated to whisker content. Nitrogen is concentrated at the interface of two composites (24% and 5% whiskers) on the fibre side of the fracture at levels of about 3 at %. The origin may be the Nicalon fibre which is known to contain approximately 0.1 at % nitrogen. Aluminium appears to be exceptionally high on the matrix side of the fracture in the 24% whisker composite. This is not seen in the other composites and may be due to the different beam voltages under which this composite was analysed relative to the first three. Carbon appears in the analysis of the trough of the 0% whisker composite at a depth of 100 nm. This is due to the sputtering beam breaking through to an adjacent interface.

The conclusion of this analysis is that there is no significant difference in the interfaces which would account for a transition from a fibrous fracture morphology (0% whiskers) to a brittle morphology (24% whiskers).

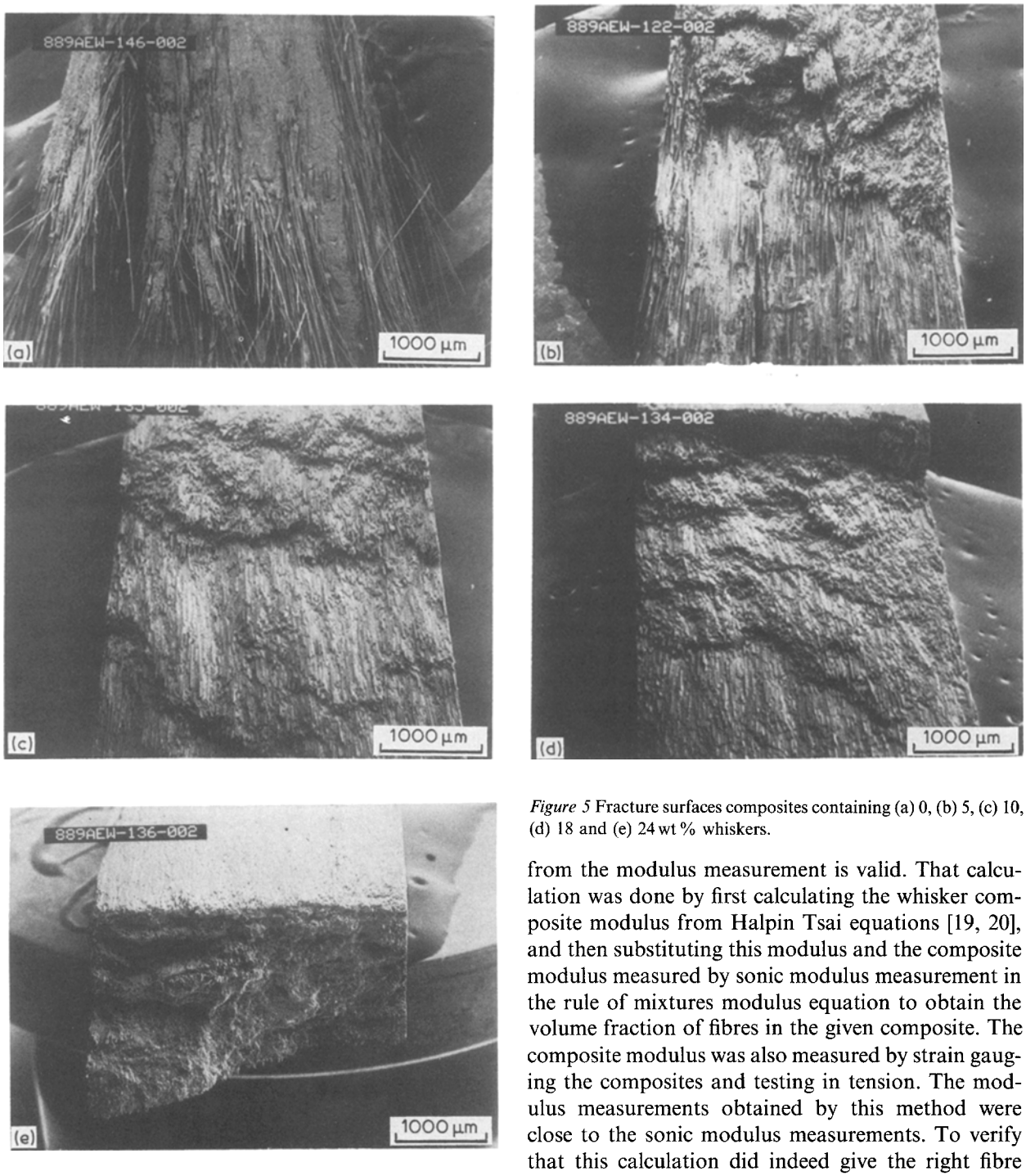

Figure 5 Fracture surfaces composites containing (a) 0, (b) 5, (c) 10, (d) 18 and (e) 24 wt % whiskers.

4.2.2. Fibre volume fraction correction

The volume fraction of the fibres in the hybrid composites may be calculated from the measured composite modulus. A careful study of the microstructure showed that the amount of porosity in the composites was not significant, and also that there was no significant variation in the amount of porosity among the various composites. Therefore, in view of those factors, the back calculation of the fibre volume fraction from the modulus measurement is valid. That calculation was done by first calculating the whisker composite modulus from Halpin Tsai equations [19, 20], and then substituting this modulus and the composite modulus measured by sonic modulus measurement in the rule of mixtures modulus equation to obtain the volume fraction of fibres in the given composite. The composite modulus was also measured by strain gauging the composites and testing in tension. The modulus measurements obtained by this method were close to the sonic modulus measurements. To verify that this calculation did indeed give the right fibre volume fraction, the strength of the fibres was calculated from the tensile strength of the composites and this known fibre volume fraction for the 0 wt % whisker composite. The calculated strength of the fibres was 1309 MPa. The fibres were extracted from the matrix by HF extractions and the strengths of the fibres were measured in tension, using the same gauge length (since fibre strengths are a strong function of gauge length) as that used for composite tension testing

TABLE I Variation in the fibre volume fraction and the composite strength with whisker percentage in the matrix

No.	Whisker percentage	Fibre volume fraction	Average ultimate strength of the composites ksi (MPa)	Predicted ultimate strength of the composites ksi (MPa)
1	0	0.45	139 (958)	139 (958)
2	5	0.455	140 (964.6)	140 (964.6)
3	10	0.42	130 (895.7)	129.7 (893.6)
4	18	0.43	116 (800)	132 (909)
5	24	0.36	50 (344)	111 (765)

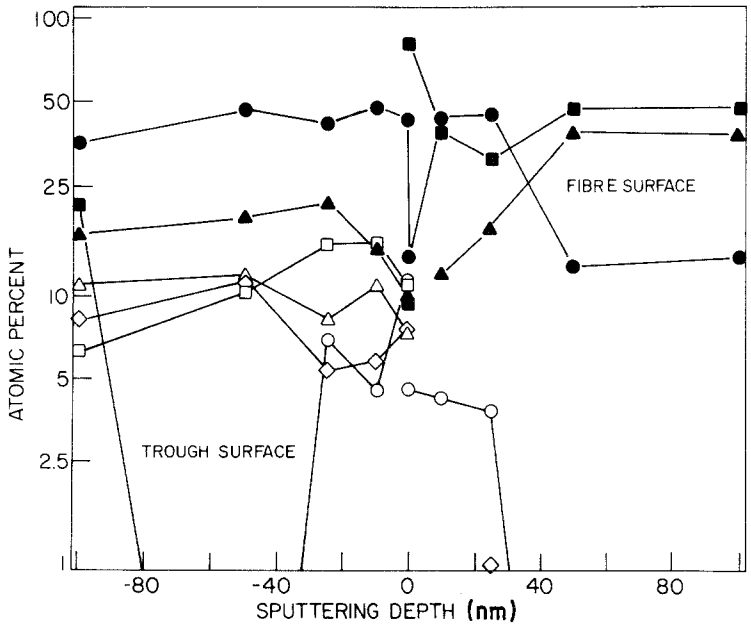

Figure 6 Auger depth profile at fibre–matrix interface for 0 wt % whisker composite. (■ carbon, ▲ silicon, ● oxygen, □ aluminium, △ barium, ◇ calcium, ○ boron)

(2.5 cm). The mean strength of the fibres was 1371 MPa. This close match in the predicted and measured strengths indicates the validity of this method of fibre volume fraction measurement.

Table I shows the variation in fibre volume fraction as a function of whisker percentage. There is a slight increase in fibre volume fraction at 5 wt % whisker loading. The fibre volume fraction decreased to 0.42 at 10 wt % whisker loading, and increased slightly to 0.43 at 18 wt % whisker loading. At 24 wt % whisker loading it dropped to 0.36. Table I also shows the predicted strengths of the composites corrected for fibre volume fraction. The predictions are obtained by calculating the fibre strengths from the known fibre volume fraction and Equation 1 for the 0 wt % fibre composite. This fibre strength and the known fibre volume fraction may be utilized to obtain the expected ultimate strength. It is evident that the predicted strengths and the experimental results are reasonably close at loadings up to 10 wt % whiskers. At 18 wt % whisker loading the strengths are substantially lower than expected. At 24 wt % whisker loading, the predicted strength is more than twice the experimentally observed strength. In view of those results, it appears that the variation in volume fraction of fibres alone does not explain the decrease in the composite strength at all the whisker loading levels.

4.2.3. Fibre damage

A careful SEM examination of the fracture surfaces was then carried out to ascertain the extent of fibre damage, if any. Figs 8a and b show micrographs of the fracture surface of the 24 wt % whisker composite. Several broken fibres are clearly seen in Fig. 8a and Fig. 8b shows a view of a fibre at higher magnification. The extensive fibre damage is quite evident. It may also be noted that the frequency of damage is high; the distance between the two large notches on the fibre is only about 3.5 μm. Such an extensive damage to the fibres would result in a significant decrease in fibre strength. This would contribute to strengths lower than could be explained by volume fraction variation of the fibres. It may be expected that the damage frequency, i.e., average distance between defects, is proportional to the whisker loading. In that case, gradually decreasing pullout lengths and a flatter

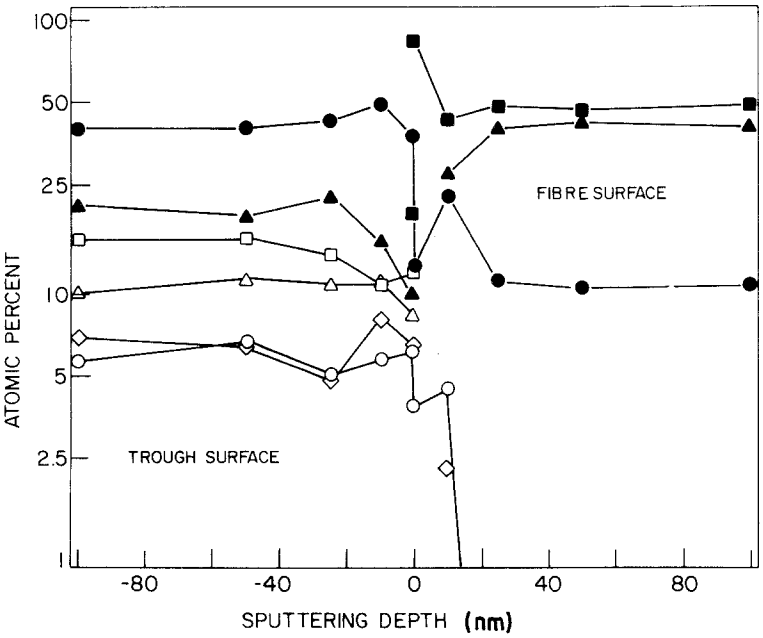

Figure 7 Auger depth profile at fibre matrix interface for 10 wt % whisker composite. (■ carbon, ▲ silicon, ● oxygen, □ aluminium, △ barium, ◇ calcium, ○ boron)

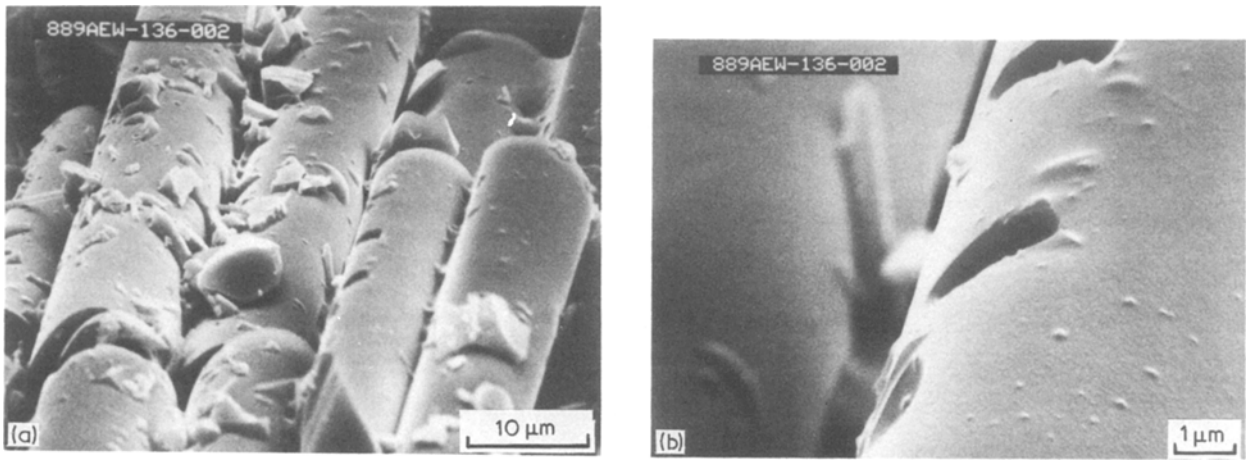

Figure 8 Fibre damage in 24 wt % whisker composite.

fracture may be expected with increases in whisker loading: at higher damage frequencies a crack may run through the material without being significantly deflected.

At very high damage frequencies, i.e., for 24 wt % whisker loading, the composite fails in a brittle manner. The fibre damage may thus explain the fracture morphologies at 18 wt % and 24 wt % whisker loadings; however, at 5 wt % whiskers and 10 wt % whiskers the strengths are at levels expected without fibre damage. At those loading levels the fibre damage must be very infrequent. However, the fracture morphologies shown in Figs 5b and c for these composites show significantly reduced pullout lengths, thereby indicating significant fibre damage. Another explanation for such a morphology may be that the mode of failure changes from compressive, shear failure (where failure occurs by buckling of the compressing surface followed by formation of a shear crack) for a 0 wt % composite to tensile failure for 5 wt % and 10 wt % composites. It is known that the interlaminar shear strength increases significantly for these hybrids, compared to the 0 wt % whisker composite, thus preventing compressive shear failures. In a compressive failure the apparent pullout lengths will be significantly longer than a tensile failure, because fibres on the compression surface are never broken during the test.

To eliminate the complication arising from the complex stress state in a bend test, tensile testing of the composite was carried out. Figs 9a and b show the ultimate and microcrack stresses and strains for the various composites.

The ultimate strength and the microcrack yield stress follow similar trends, as seen from flexural strength measurements. The microcrack yield strains also show an optimum around 10 wt % whisker loading. The ultimate strain or strain to failure, however, shows a continuous decline with increasing whisker loading. Even at 5 wt % whisker loading, the ultimate failure strain has declined to 0.6% from 0.85% for 0 wt % composite. This clearly indicates fibre damage even at 5 wt % whiskers. From the ultimate strain curve it is clear that fibre damage is progressively increased with increased whisker loading. The fibre damage thus is clearly the cause of the observed fracture surface morphology with increasingly shorter pullout lengths at 5 and 10% and higher whisker loadings.

In spite of the whisker induced damage, the strengths at 5 wt % and 10 wt % whisker loadings are not decreased. A plausible explanation for this behaviour is as follows: at 5 and 10 wt % loadings the damage frequency is such that the length of the fibre between two damaged sites is enough to attain average fibre stress close to that of the average fibre stress in a continuous fibre composite. Some support for this contention is obtained from the following analysis. We can calculate the load transfer length of the fibre from the following equation

$$\frac{\sigma_f}{2\tau_m} = \left(\frac{1}{d}\right)_c \tag{8}$$

The interfacial shear strength $\tau_m = 235$ MPa is taken from Mandell's [18] work on 1723/Nicalon system. Since the chemical nature of the interface does not change, the same bond strengths have been assumed for hybrid composites. The extracted fibre strength of 1371 MPa gives a load transfer aspect ratio of $\simeq 3$. From the measured average diameter of the Nicalon fibre of 7.3 μm, the load transfer length may be calculated to be $\simeq 22\,\mu$m.

Hence, the ratio of σ_f/σ_{max} i.e. average fibre stress to maximum fibre stress of 0.9 may be achieved at fibre lengths of 110 μm; that of 0.95 at fibre length of 220 μm [20]. As the ratio approaches 1, continuous fibre behaviour is approached. Micrographs of the failure surfaces of the specimen broken in tension were taken and average pullout length was measured. At 5, 10, and 18 wt % whiskers the average length was 0.562 mm, 0.48 mm and 0.14 mm, respectively. No measurable pullout was seen at 24 wt % whiskers.

It is reasonable to assume that the fibre length between two adjacent damage sites will be larger than the pullout length. Based on the calculated stress ratios, it may be predicted that ultimate strengths of 5 and 10 wt % whisker hybrids should be close to the undamaged fibre composites. The strengths at 18 wt % whiskers would be less than the strengths obtained with undamaged fibres. At 24 wt % whiskers

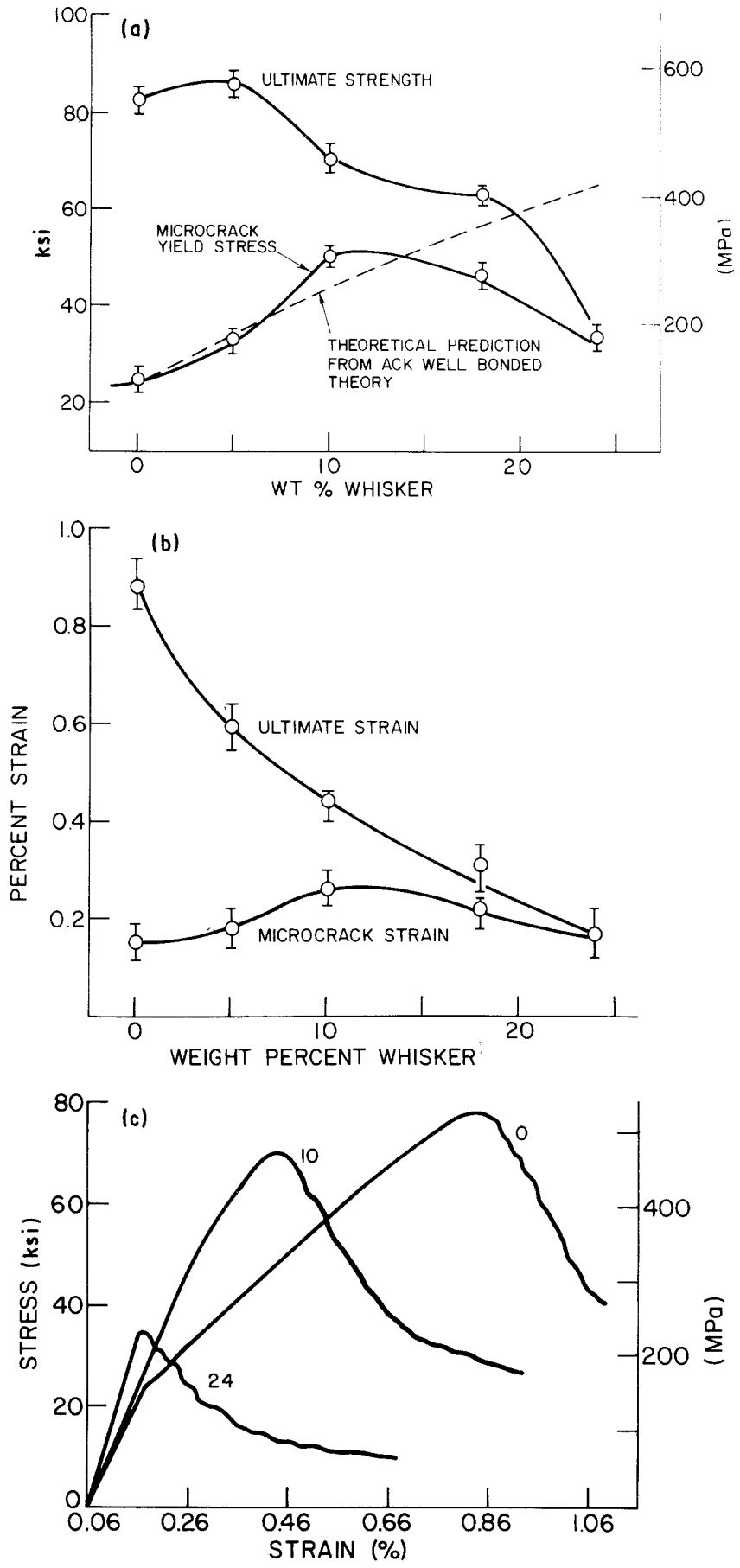

Figure 9 (a) Tensile ultimate strength and microcrack yield stress of hybrid composites as a function of whisker loading. (b) Ultimate failure strain and microcrack measured in tension. (c) Tensile stress–strain curves for various hybrid composites (the numbers adjacent to curves indicate whisker loading level).

the composite essentially acts as a short fibre composite. Though based on several simplifying assumptions, this analysis appears to explain the experimental data.

Fig. 9a also shows the variation in microcrack yield stress with whisker loading. The theoretical and experimental predictions match very well at 5 wt % whisker loading. The theory, however, slightly underestimates the improvements in microcrack stress at 10 wt % whiskers. At higher whisker loadings, however, the experimental microcrack stresses are significantly lower than predicted. This is an expected

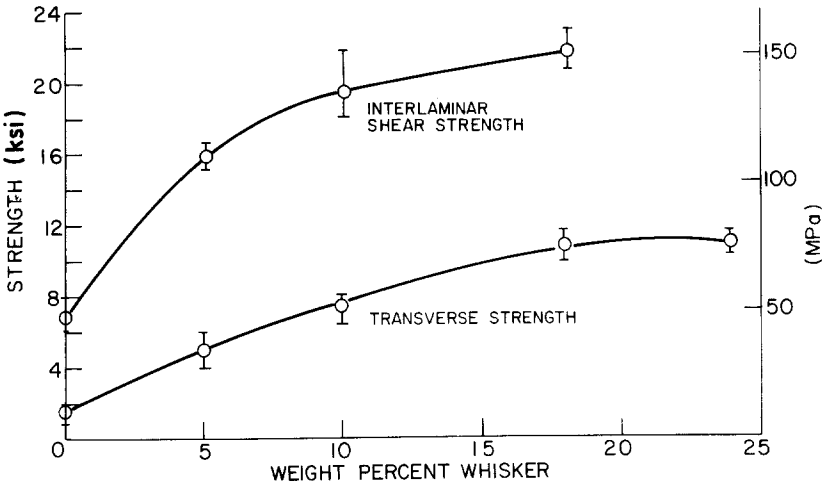

Figure 10 Transverse strength and interlaminar shear stress as a function of whisker percentage.

behaviour based on the fibre damage model presented earlier. At 18 wt % whisker loading and beyond, the composites do not behave as continuous fibre composites and, hence, the theory is not applicable. Fig. 9c shows the tensile stress–strain curves for 0, 10, and 24 wt % whisker hybrid composites. In spite of significant fibre damage at high whisker loadings, the composite failure is still not catastrophic.

4.3. The interlaminar shear strength (ILSS) and the transverse strength

Fig. 10 shows the variation of ILSS and transverse strength as a function of whisker percentage. Both the transverse strength and the interlaminar shear strength increase with increasing whisker percentage. The transverse strength increases from 10.3 MPa to 53.7 MPa and the interlaminar strength increases from 44.8 MPa to 134.35 MPa as whisker loading is increased from 0 wt % to 10 wt % whiskers.

Based on all the data presented so far, a 10 wt % whisker loading gives the optimum composite in the 1723/Nicalon system.

5. Conclusions

This work has verified the theoretical prediction that the matrix microcracking stress of a fibre reinforced ceramic matrix composite may be increased by inclusion of an additional reinforcing phase, such as silicon carbide whiskers. The ultimate strength was lower than the theoretical expectations at whisker loadings above about 10 wt % and has been ascribed to fibre damage by the whiskers.

Improvement in the microcracking stress is important because σ_{mcy} is the practical engineering limit of the composite, and represents the stress at which embrittlement under high temperature oxidizing conditions begins. This hybrid approach thus promises more reliable high temperature ceramic matrix composites with higher design stresses.

An additional benefit of the whisker reinforced matrix is a doubling or tripling of the transverse strength and the interlaminar shear strength. These properties are often the design limiting properties of high temperature composites, especially during thermal transients such as during ignition of a gas turbine engine.

References

1. J. SUMMERSCALES and D. SHORT, *Composites* **9** (1978) 157–166.
2. B. HARRIS and A. R. BUNSELL, *Composites* **6** (1975) 197–201.
3. M. B. GRUBER and T. CHOU, *Polym. Composites* **4** (1985) 265–269.
4. N. L. HANCOX, *J. Mater. Sci.* **19** (1984) 1969–1973.
5. H. FUKUNAGA and T. W. CHOU, *J. Reinf. Plast. Comp.* **3** (1984) 145–160.
6. S. K. CHATURVEDI and C. T. SUN, *Int. J. Fracture* **24** (1984) 179–188.
7. R. F. FORAL and W. D. HUMPHREY, *AIAA J.* **22** (1984) 111–116.
8. T. ISHIKAWA and T. S. CHOU, *J. Mater. Sci.* **18** (1983) 2260–2268.
9. K. M. PREWO and J. J. BRENNAN, *ibid.* **15** (1980) 463–468.
10. J. J. BRENAN and K. M. PREWO, *ibid.* **17** (1982) 2871–2883.
11. K. CHYUNG, M. P. TAYLOR and R. L. STEWART, "Refractory Glass Ceramic Matrices and Their Composites Reinforced with SiC Fibers". Presented at 8th Annual Meeting of American Ceramic Society, May 1985, Cincinnati, OH.
12. R. L. STEWART, K. CHYUNG, M. P. TAYLOR and R. F. COOPER, "Fracture Mechanics of Ceramics", Vol. 7 (Edited by R.C. Bradt, D.P.H. Hasselman, A.G. Evans and F.F. Lange) Plenum Press (1986).
13. K. P. GADKAREE and K. C. CHYUNG, *Amer. Ceram. Soc. Bull.* **65** (1986) 370–376.
14. *Idem*, "Stuffed Cordierite Matrix Whisker Composites". Presented at 88th Annual Meeting of American Ceramic Society, April 1986, Chicago, IL.
15. K. P. R. REDDY and K. P. GADKAREE, "Mechanical Properties of Whisker Reinforced Glass". Proceedings of XIV International Congress on Glass, Vol. III, pp. 270–277 (Indian Ceramic Society (1986).
16. J. AVESTON, G. A. COOPER and A. KELLY, "Single and multiple fracture", pp. 15–26 in *The Properties of Fibre Composites*, National Physics Laboratory Conf. Proc., IPC Science and Technology Press, Surrey, England (1971).
17. J. AVESTON and A. KELLY, *J. Mater. Sci.* **8** (1973) 352.
18. J. F. MANDELL, K. C. C. HONG and H. G. GRANDE, Ceramic Science and Engineering Proceedings, American Ceramic Society **8** (1987) 937–940.
19. L. E. NIELSON, in "Mechanical Properties of Polymers and Composites," Vol. 2 (Marcel Dekker, New York, 1974) p. 407.
20. B. D. AGARWAL and L. J. BRAUTMAN, "Analysis and Performance of Fiber Composites," (Wiley Interscience, New York, 1980).

Received 2 October 1987
and accepted 26 January 1988